SAND2023-04585C

Society for Experimental Mechanics
Annual Conference
June 5th, 2023

Considerations for the Identification of Elasto-Plastic Material Model Parameters

Samuel Fayad[a], Dr. Tom Seidl[b], Dr. Elizabeth Jones[b], Dr. Phil Reu[b], Dr. John Lambros[a]
[a]University of Illinois, Urbana IL
[b]Sandia National Laboratories, Albuquerque NM

Funding acknowledgement: Sandia National Laboratories is a multimission laboratory managed and operated by National Technology & Engineering Solutions of Sandia, LLC, a wholly owned subsidiary of Honeywell International Inc., for the U.S. Department of Energy's National Nuclear Security Administration under contract DE-NA0003525. This paper describes objective technical results and analysis. Any subjective views or opinions that might be expressed in the paper do not necessarily represent the views of the U.S. Department of Energy or the United States Government.

We would also like to acknowledge the Sandia-granted award #2202897 and the University of Illinois grant #101852 for funding this

Sandia National Laboratories is a multimission laboratory managed and operated by National Technology & Engineering Solutions of Sandia, LLC, a wholly owned subsidiary of Honeywell International Inc., for the U.S. Department of Energy's National Nuclear Security Administration under contract DE-NA0003525.

Finite Element Analysis and Material Models

FEA to analyze stress and strain that cannot be analytically studied

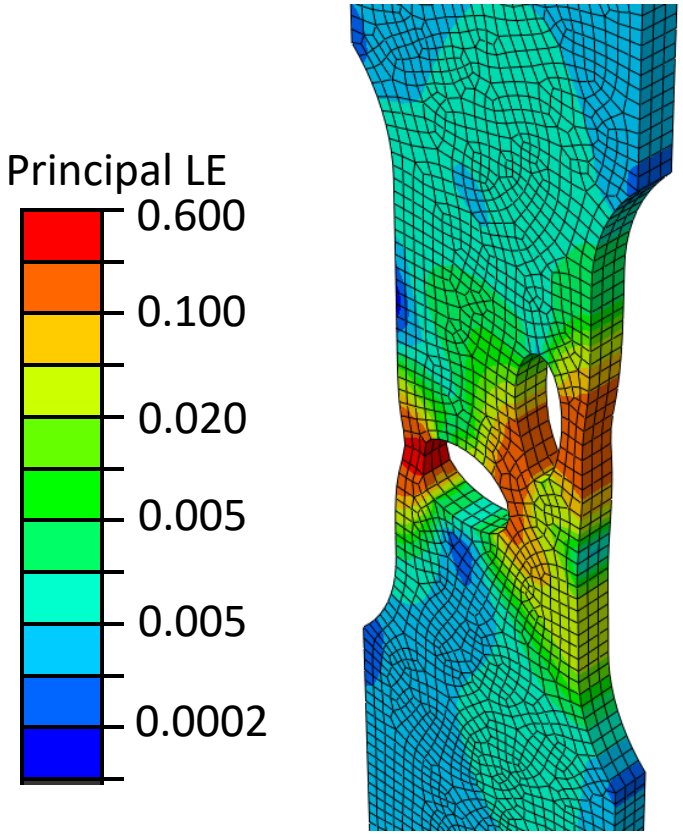

Perforated sheet metal under uniaxial loading

Material behavior like hardening and yield dictated by material model parameters

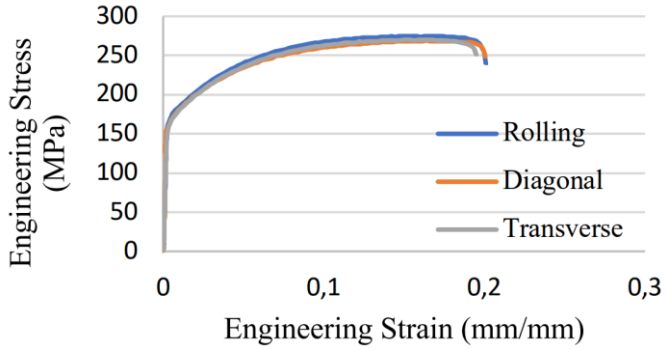

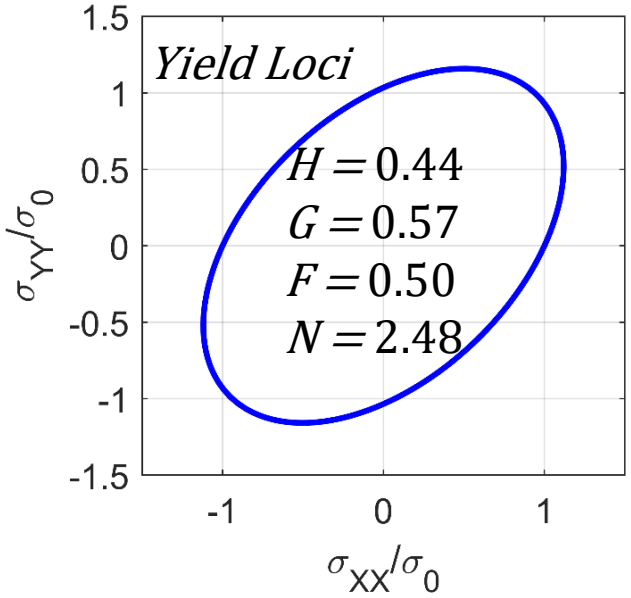

(A Ünlü. et al. 2020)

Experiments needed to determine material parameters

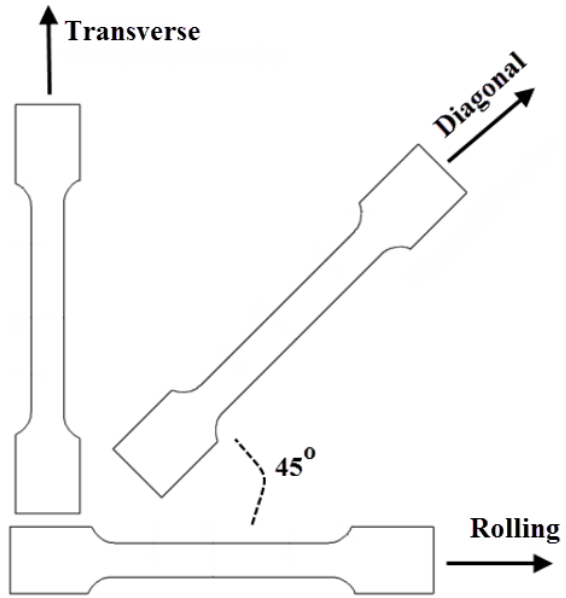

(A Ünlü. et al. 2020)

Experimentation and Calibration of Material Models using Full-Field Methods

Background:

More advanced calibration techniques (Pierron 2023) are gaining popularity because:

- Boundary conditions can be measured
- The measurement data is richer
- Complex stress states can be achieved
- Experimental parameter space is wider

Problem:

- Errors in the experiment, measurements, and model assumptions

Goal:

- Study the role of these errors in the parameter identification

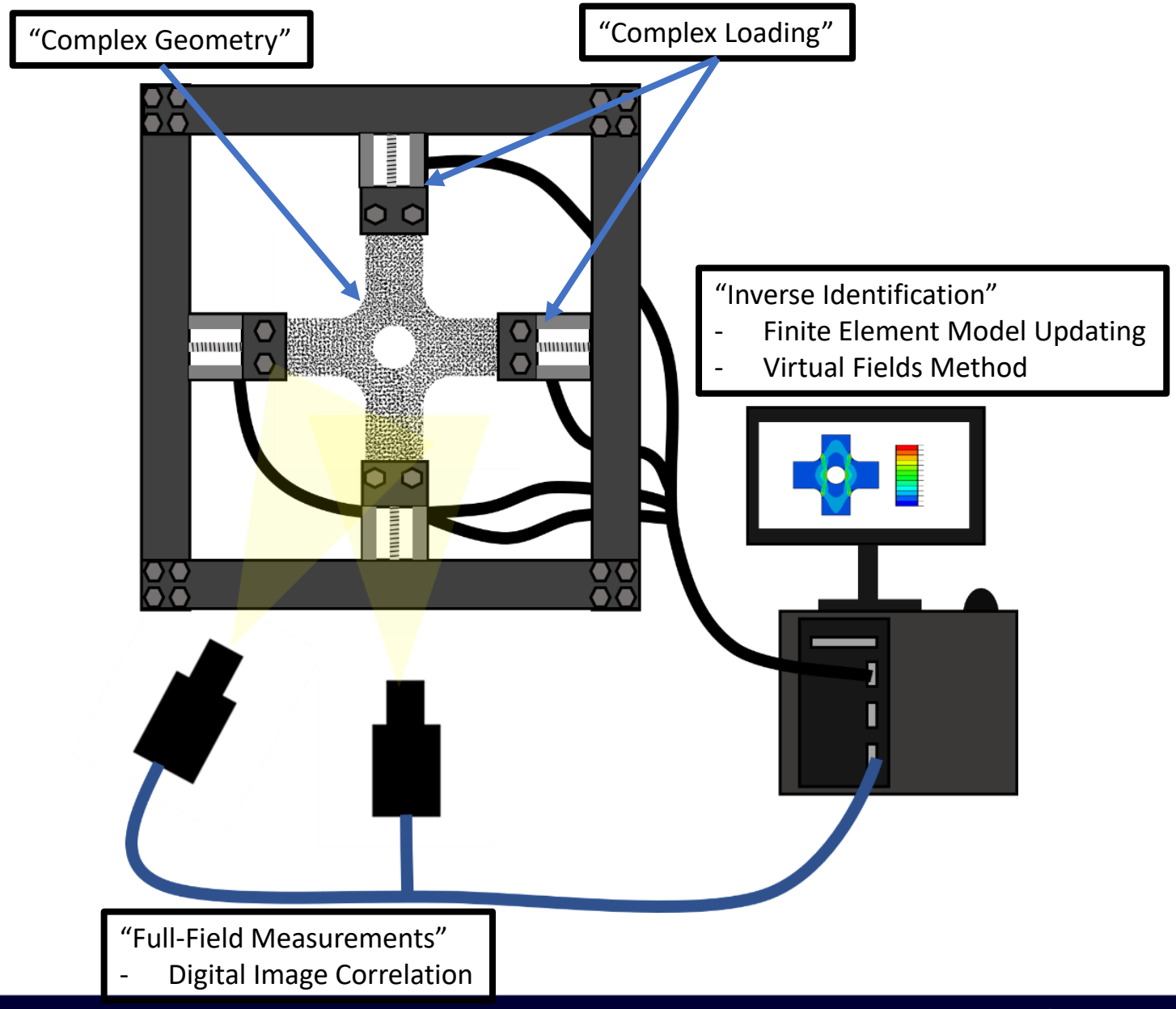

Finite Element Model Updating (FEMU)

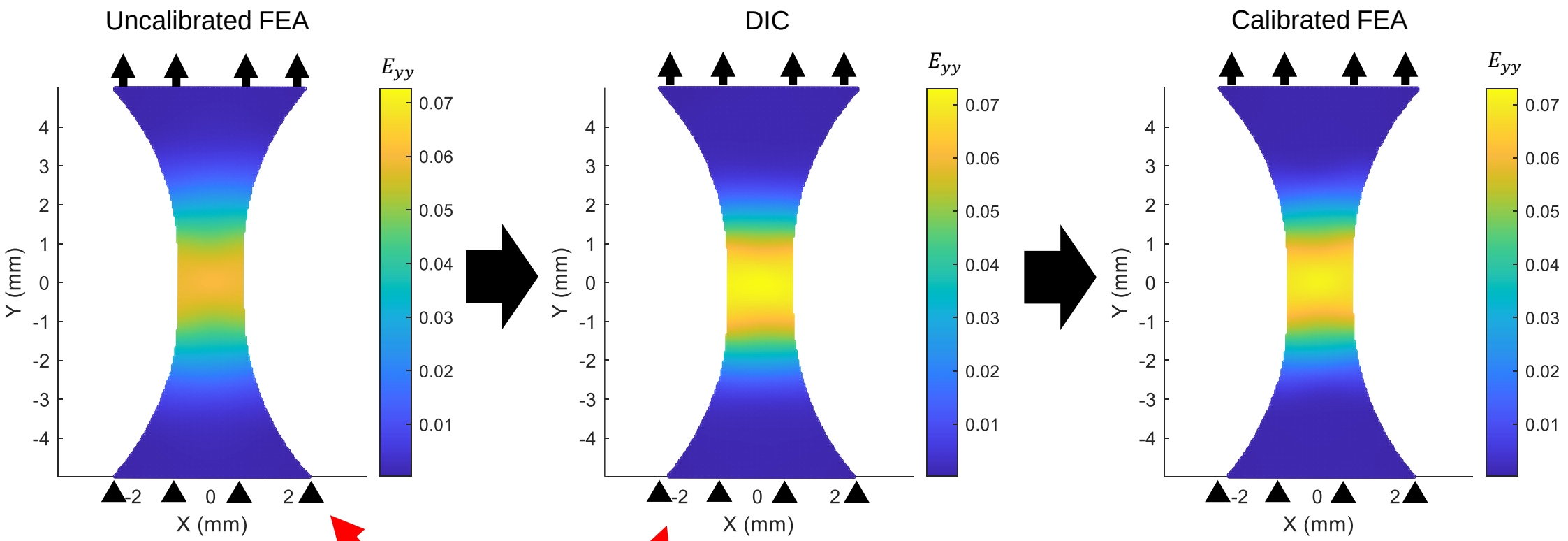

FEMU Cost Function

$$\boldsymbol{\rho}^* = \min_{\boldsymbol{\rho}} \frac{1}{N_\epsilon} \Sigma_{i=1}^{N_\epsilon} [\boldsymbol{q}_c(\boldsymbol{\rho}) - \boldsymbol{q}_m]^2$$

Solved via Gauss-Newton method (F. Mathieu et al. 2015)

$\boldsymbol{q}_m$: Experimentally measure quantity, e.g. displacement/strain
$\boldsymbol{q}_c$: the FEA computed quantity
$\boldsymbol{N}_\epsilon$: number of total sample points
$\boldsymbol{\rho}$: the material model parameter vector

Error Sources and Considerations

(Presenting initial results)

(Other things to consider)

Experimental/Metrological

- DIC filtering biases
- Misalignment between DIC and FE model
- Non-ideal boundary conditions
- DIC errors such as image noise, pattern-induced bias, subpixel interpolation bias whose effects are small on calibration (Fayad 2022)

Model Form Error

- Assumptions of Plane Stress (Future work)
- Selection of Empirical Models (Future work)

Inverse Technique

- Choice of Cost Function quantities for the Inverse Method (Future work)

Experimental/Metrological

- **→DIC filtering biases←**
- Misalignment between DIC and FE model
- Non-ideal boundary conditions
- DIC errors such as image noise, pattern-induced bias, subpixel interpolation bias whose effects are small on calibration (Fayad 2022)

Model Form Error

- Assumptions of Plane Stress (Future work)
- Selection of Empirical Models (Future work)

Inverse Technique

- Choice of Cost Function quantities for the Inverse Method (Future work)

Factors affecting spatial resolution: FEA and DIC

FEA is mainly affected by element size

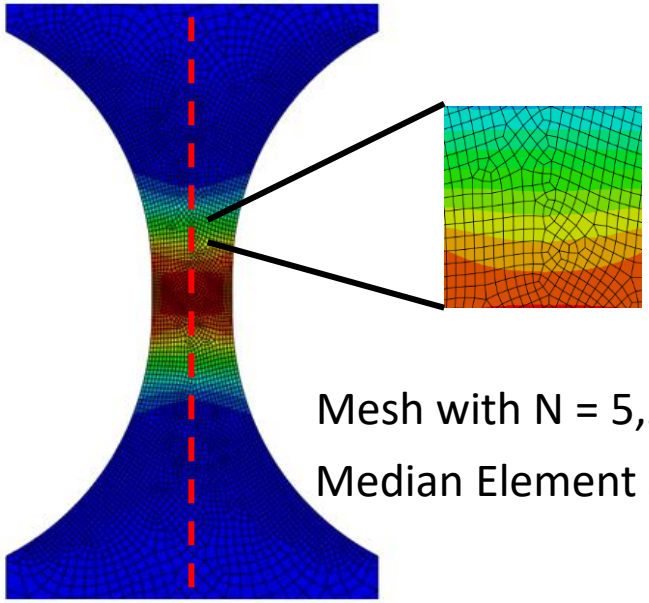

Mesh with N = 5,202 elements

Median Element Size 0.01 mm^2

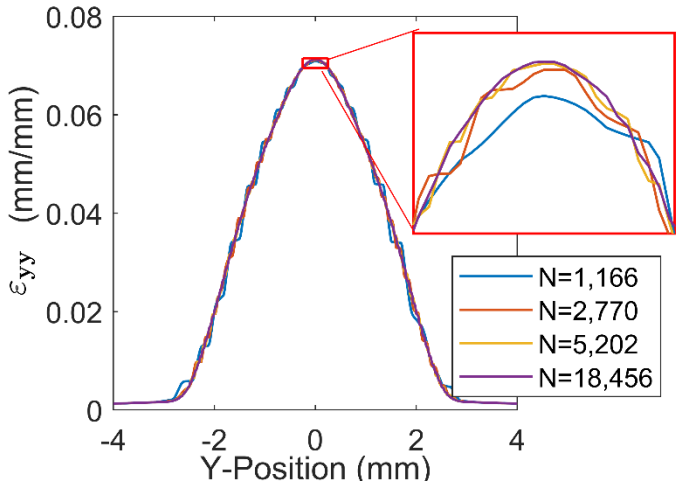

DIC is affected by the subset size and virtual strain gage size

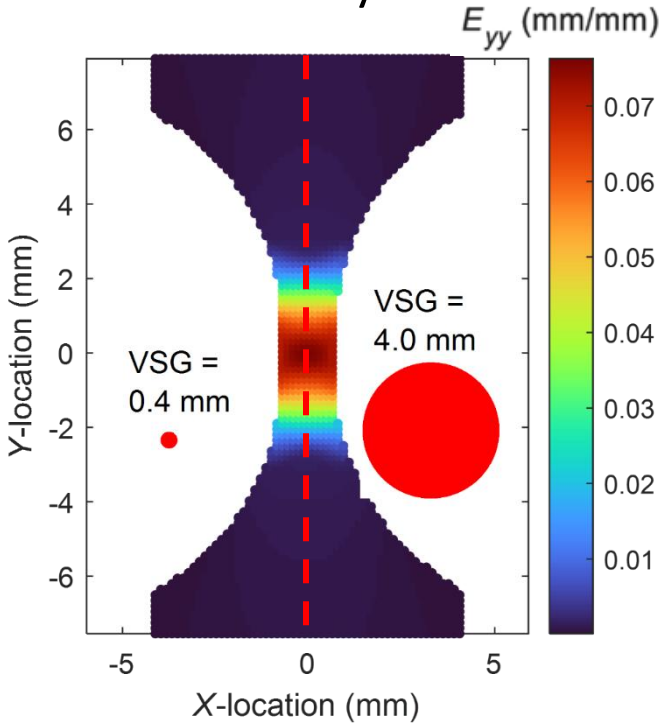

Fayad, S. S., et al. Exp. Mech. (2022): 1-18.

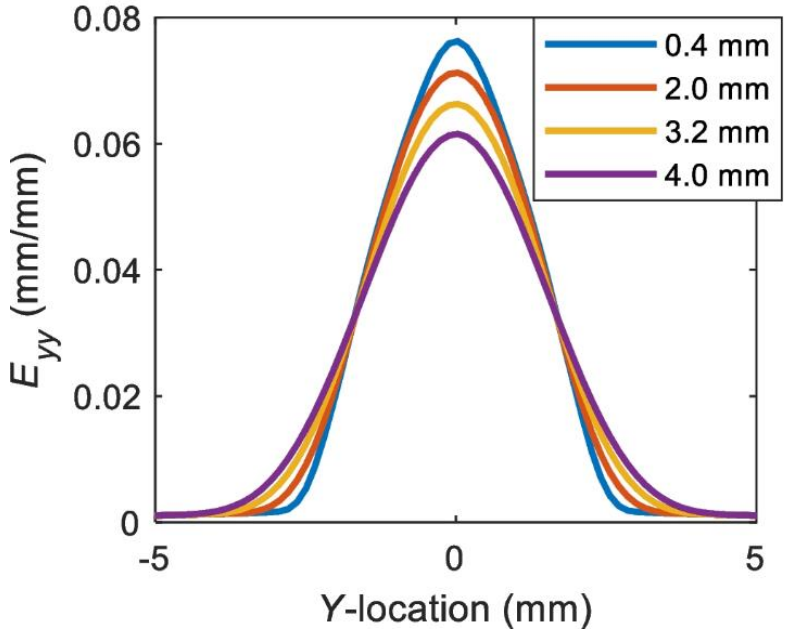

Direct-levelling procedure for 2D DIC

Steps:

1. Apply DIC grid to the FEA.

FEA Displacement

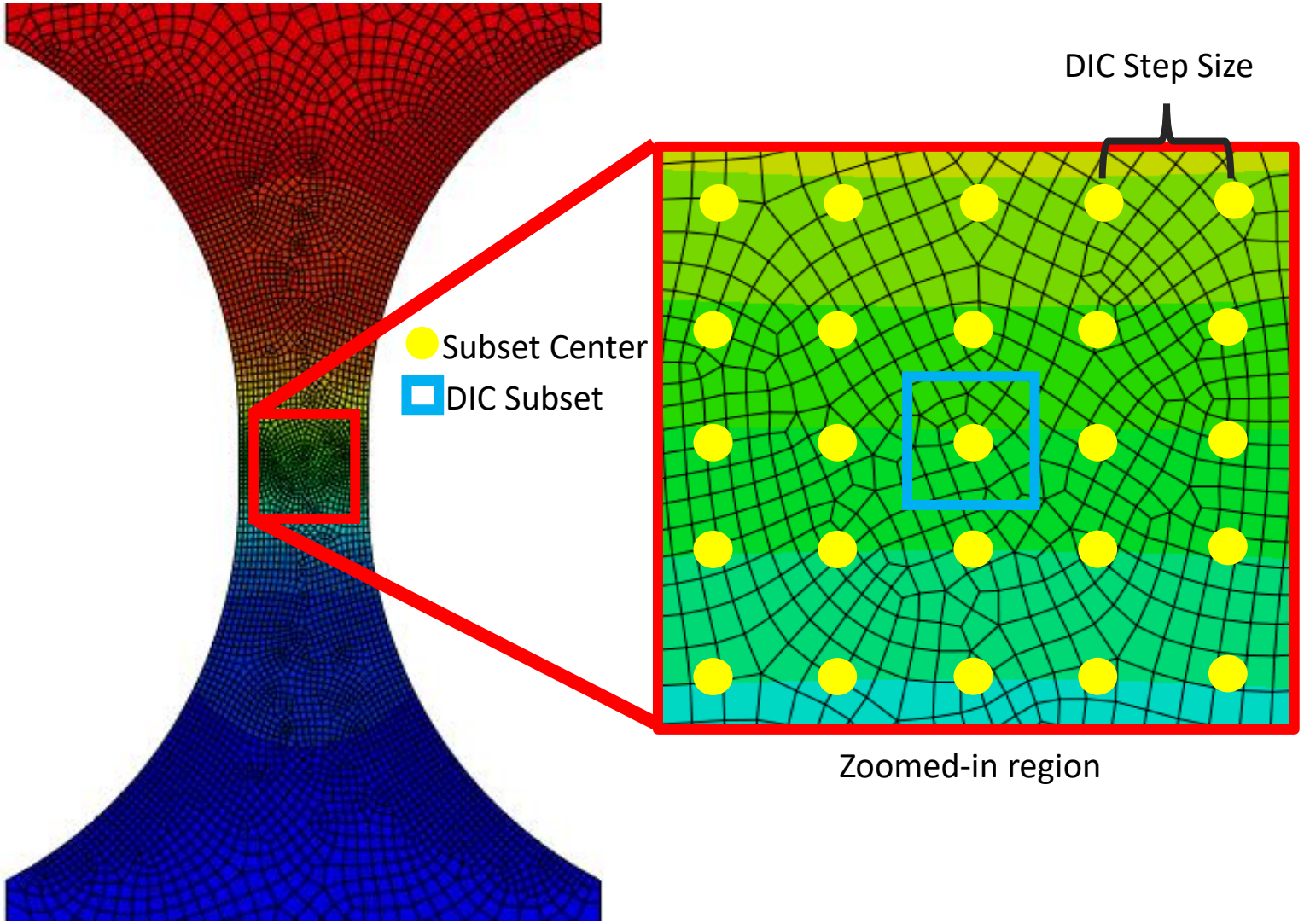

Direct-levelling procedure for 2D DIC

Steps:

1. Apply DIC grid to the FEA.
2. Interpolate the FEA nodal displacement to the image pixel locations for each subset.
3. Fit DIC subset shape function e.g. affine, quadratic to estimate the DIC-filtered displacement

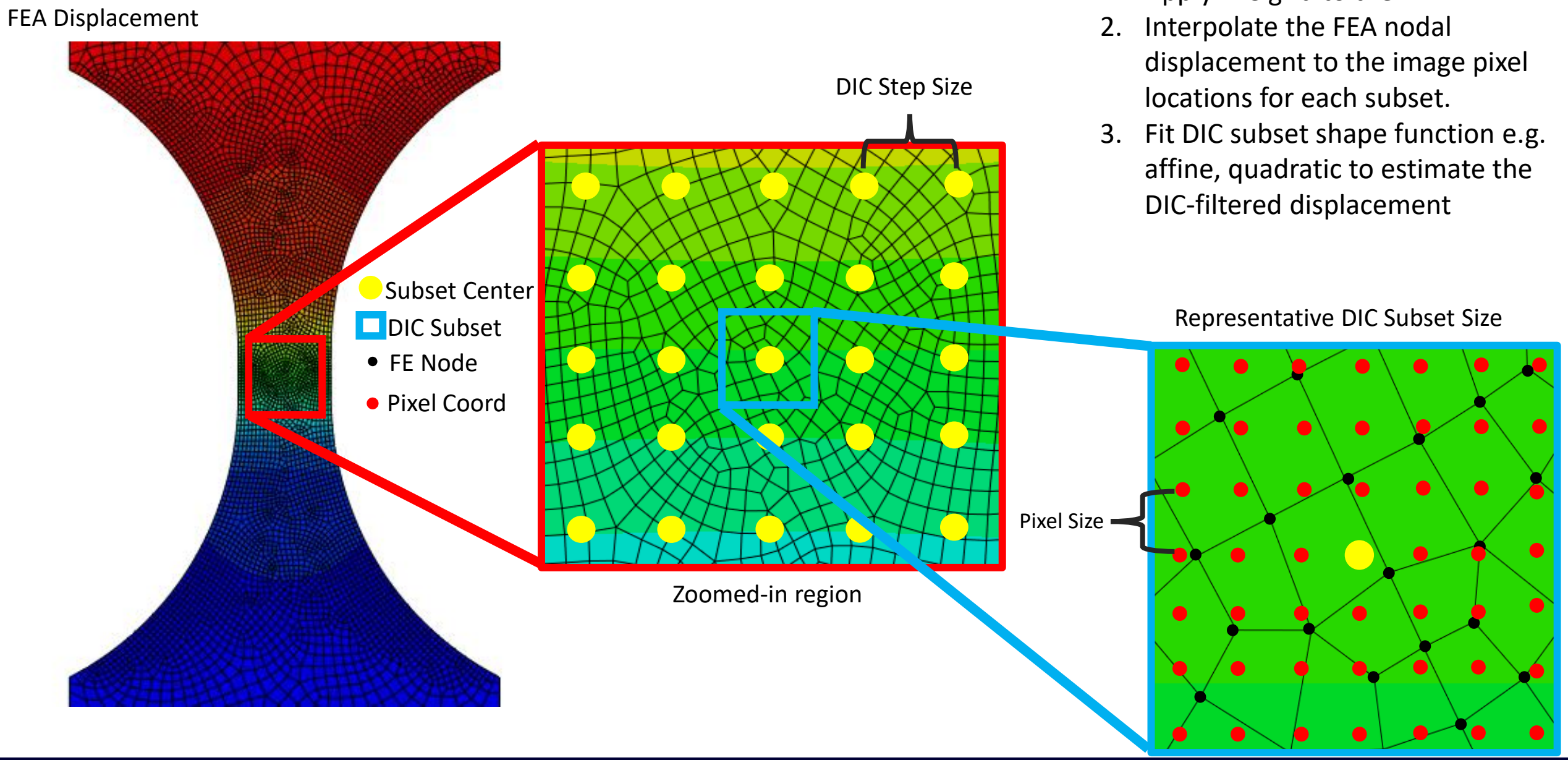

Direct-levelling procedure for 2D DIC

FEA Displacement

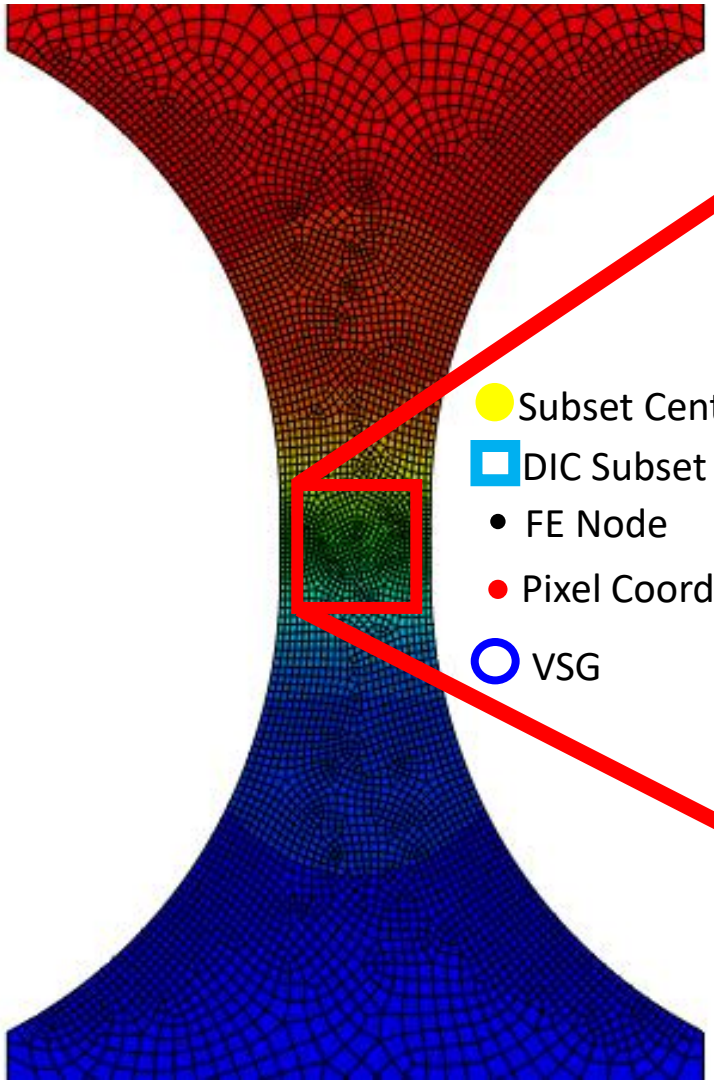

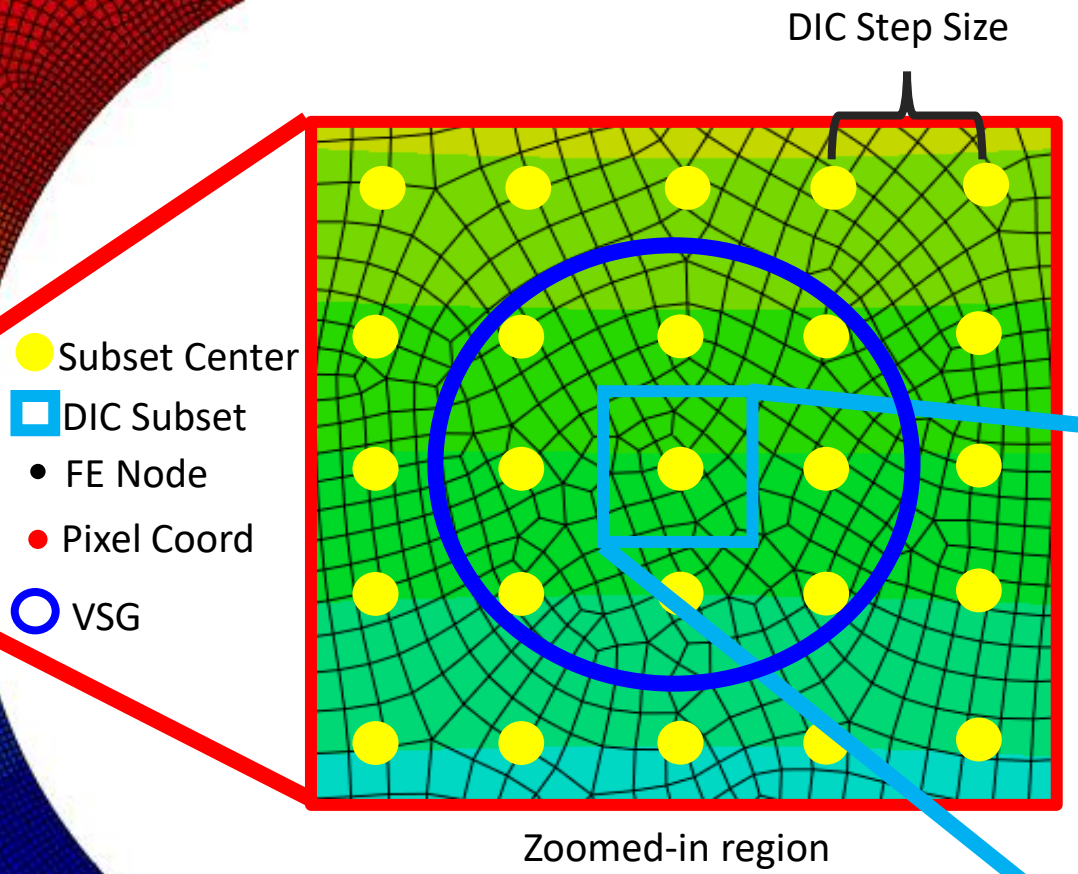

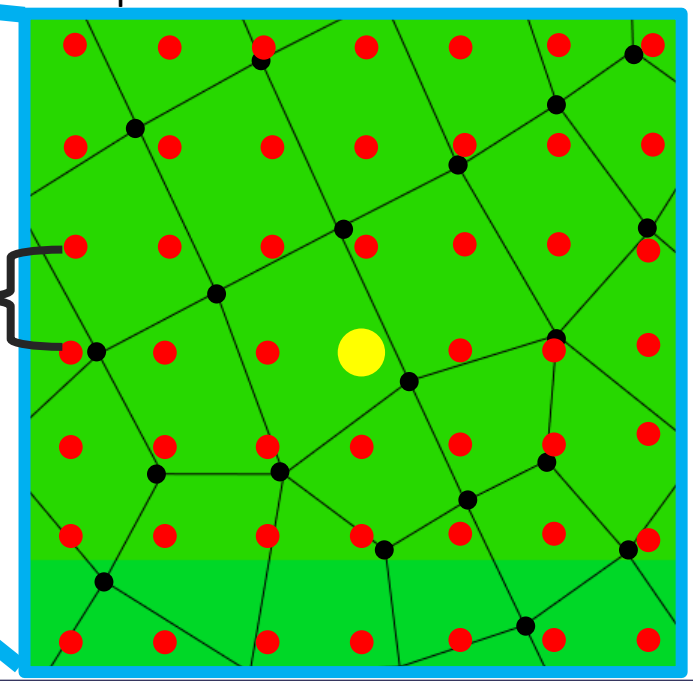

Steps:

1. Apply DIC grid to the FEA.
2. Interpolate the FEA nodal displacement to the image pixel locations for each subset.
3. Apply DIC subset shape function e.g. affine, quadratic
4. Apply the DIC strain shape function to the subset displacements within the VSG

The work done by [Lava et al. 2020] accounts for some image-based errors in stereo DIC

Experimental/Metrological

- **DIC filtering biases→ Levelling the FE Model**
- Misalignment between DIC and FE model
- Non-ideal boundary conditions
- DIC errors such as image noise, pattern-induced bias, subpixel interpolation bias whose effects are small on calibration (Fayad 2022)

Model Form Error

- Assumptions of Plane Stress (Future work)
- Selection of Empirical Models (Future work)

Inverse Technique

- Choice of Cost Function quantities for the Inverse Method (Future work)

Levelling example using synthetic “experimental” data

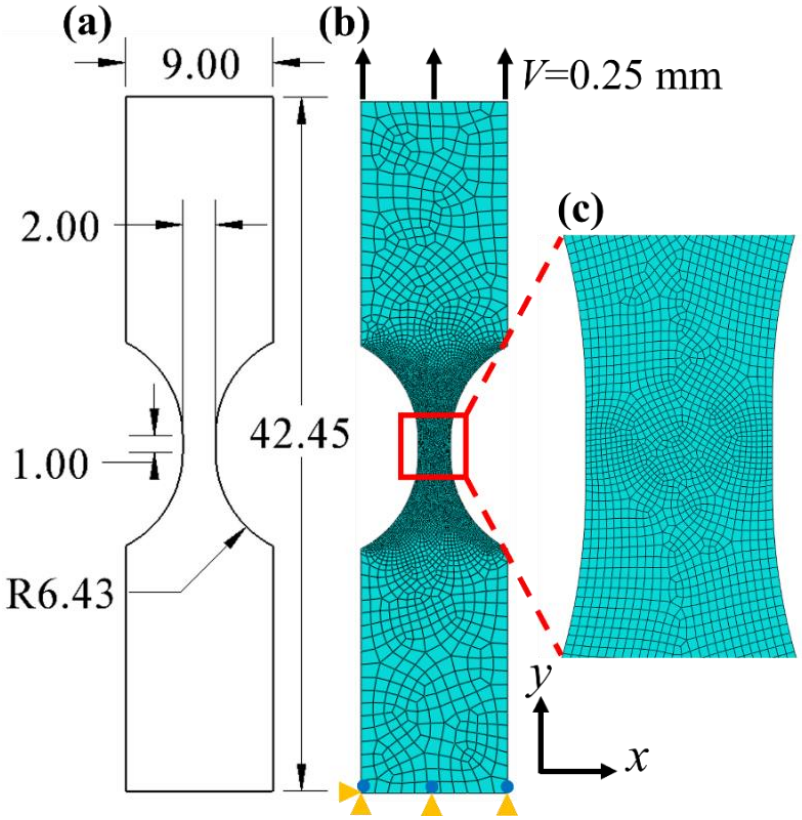

5202 CPS4 element plane-stress FE model

Material hardening is given by the power law:

$$\sigma_y = \sigma_0 + B(\bar{\varepsilon}^p)^n$$

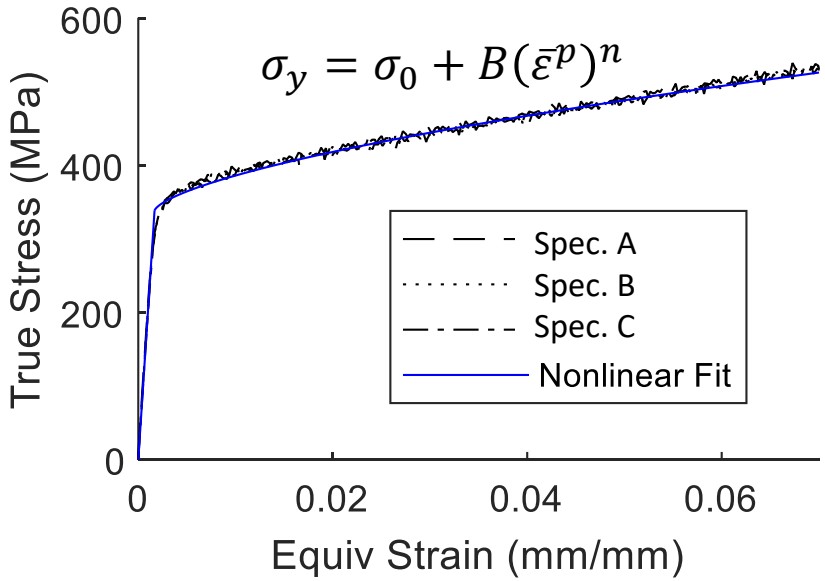

Parameter	Young’s Mod. (GPa)	ν	σ_0 (MPa)	B (MPa)	n
Ground Truth	200	0.29	339	1,070	0.645
Initial Guess	N/A (fixed)	N/A (fixed)	305	1,180	0.581

*Ground-truth parameters provide a baseline to measure identification accuracy

FEMU Analysis using Synthetic DIC Data

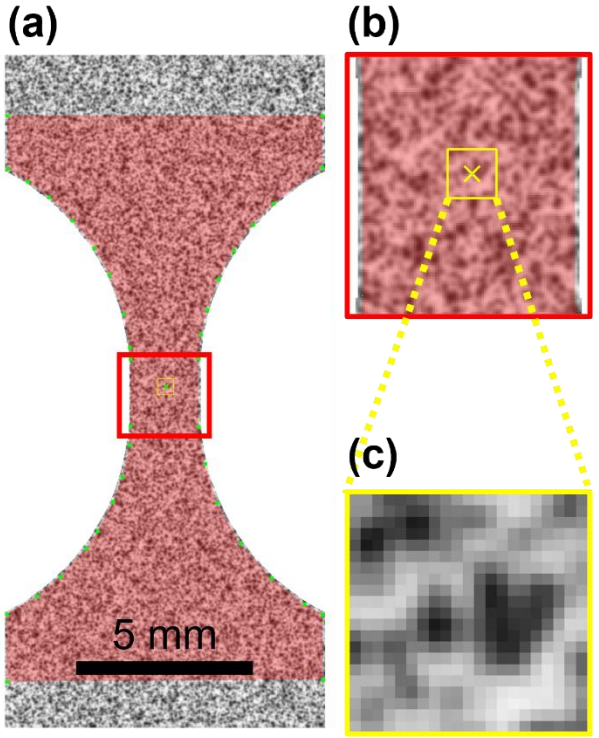

Synthetically generated images from (BSpeckleRender Blaysat, B. 2018)

DIC Software	Subset Size	Step Size	Shape Function	Criterion	Image Interpolant
MatchID	21 px	7 px	**Quadratic**	NSSD	**Bicubic Spl.**

Hardening Law

$$\sigma_y = \boldsymbol{\sigma_0} + \boldsymbol{B}(\bar{\varepsilon}^p)^{\boldsymbol{n}}$$

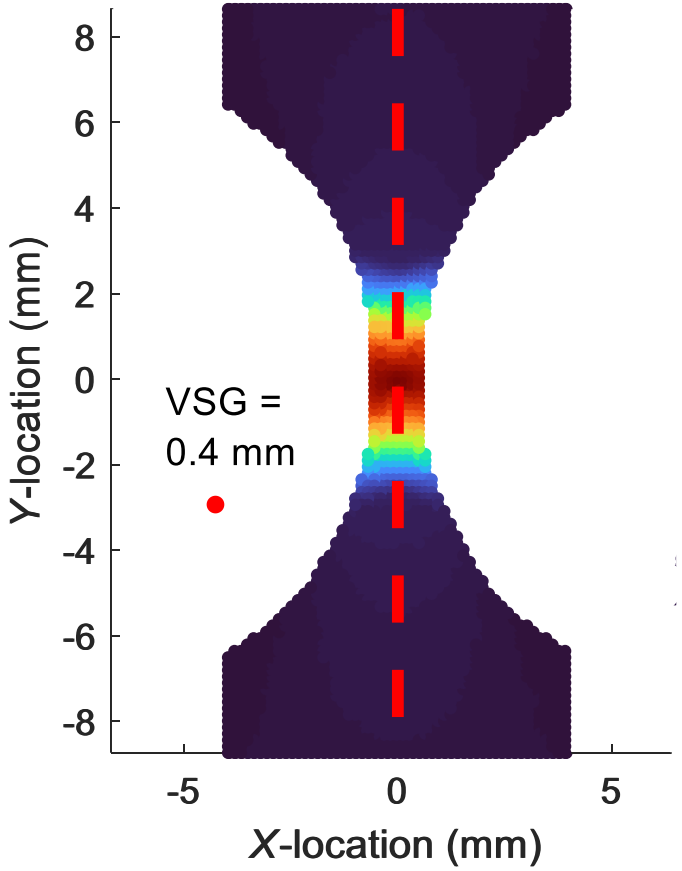

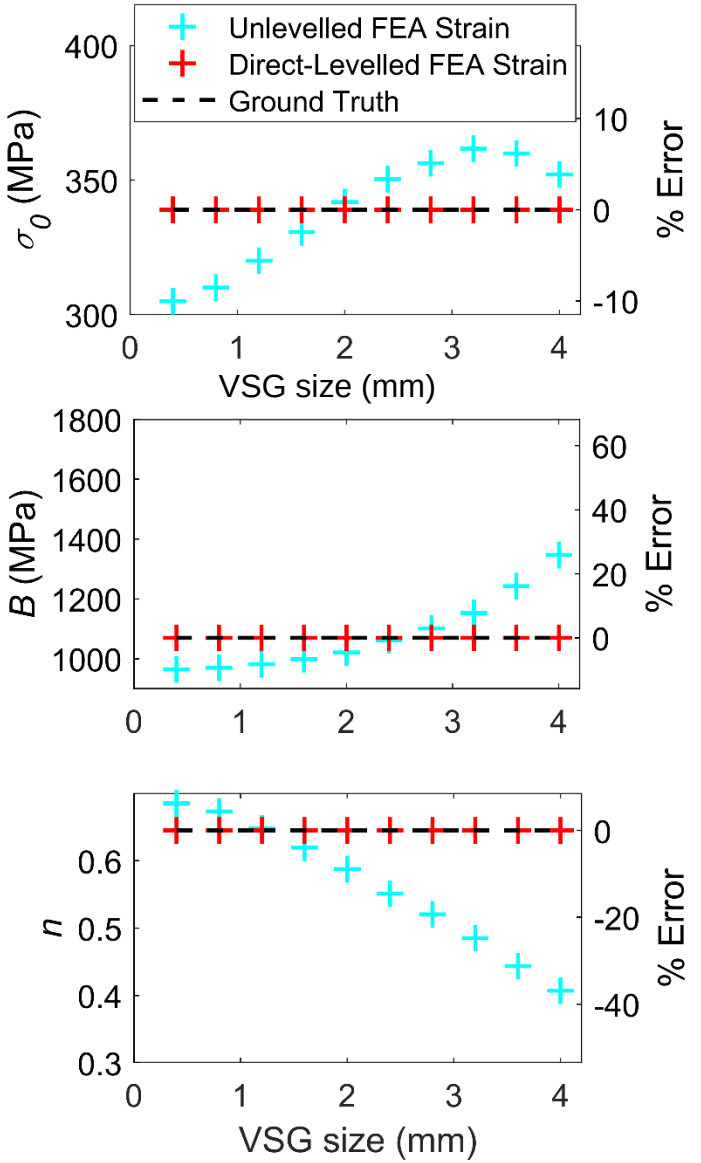

Work published in (Fayad 2022)

Experimental

- DIC filtering biases
- **→Misalignment between DIC and FE model←**
- Non-ideal boundary conditions

Metrological

- DIC errors such as image noise, pattern-induced bias, subpixel interpolation bias whose effects are small on calibration (Fayad 2022)

Model Form Error

- Assumptions of Plane Stress (Future work)
- Selection of Empirical Models (Future work)

Inverse Technique

- Choice of Cost Function quantities for the Inverse Method (Future work)

Calibration Error Source: Misalignment Between DIC and FEA

Typical point cloud alignment algorithm:

$\boldsymbol{T}^* = \underset{\boldsymbol{T}}{argmin}[\boldsymbol{X}_{DIC}\boldsymbol{T} - \boldsymbol{X}_{FEA}]^2$ (Stander 2017)

$\boldsymbol{X}$: Point cloud locations

$\boldsymbol{T}$: Transformation matrix

Misalignment due to:

- Poor registration method
- Lens distortion
- Lack of DIC data near edges
- Imprecise fiducial marking

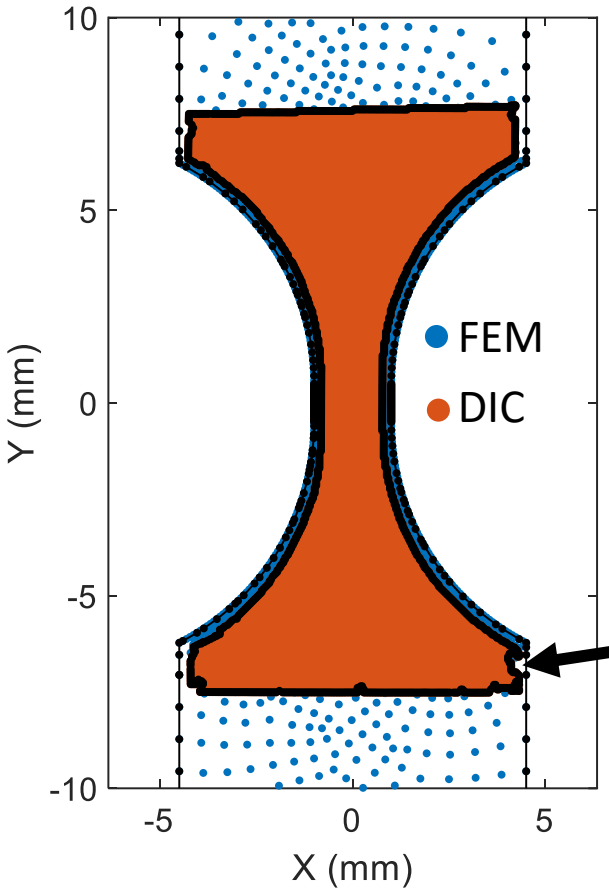

Dropped points

Step size of 5 pixels or 0.0408 mm, misalignment could be similar order of magnitude

Lens Distortion

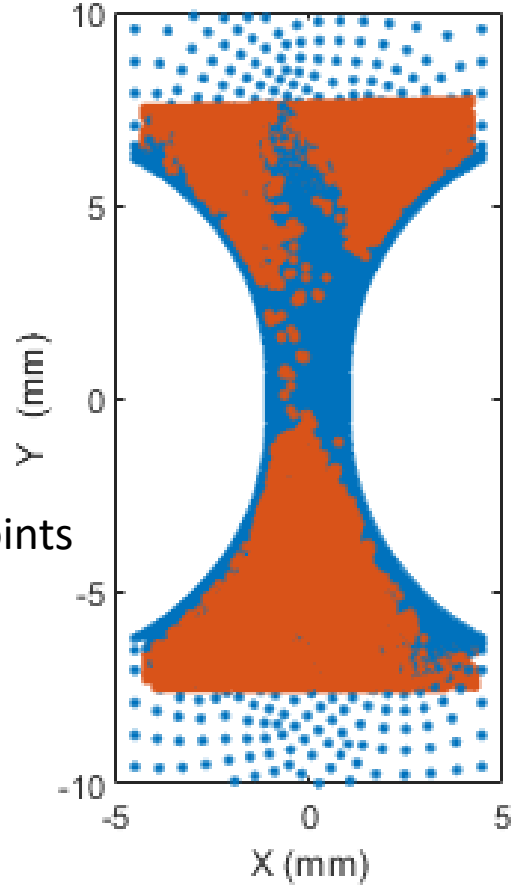

Identification Error Magnitude due to Misalignment

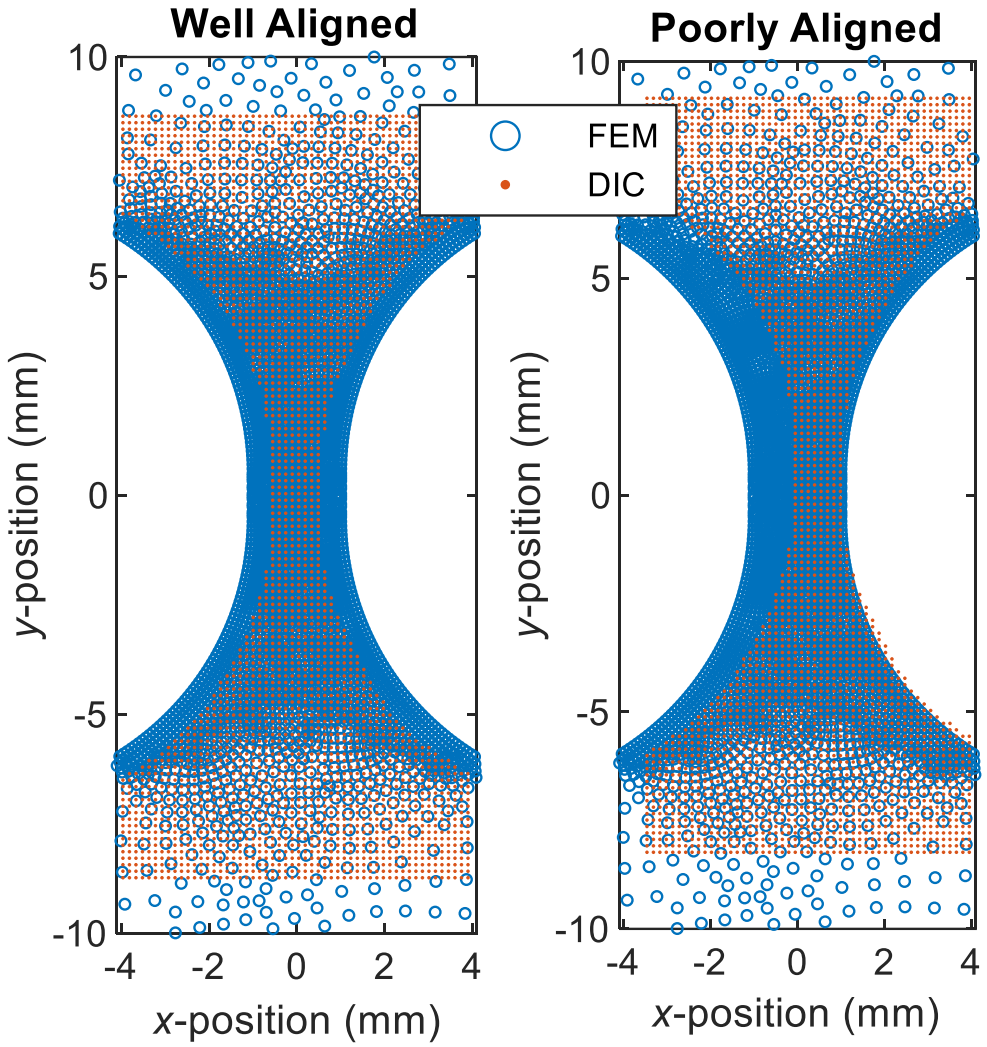

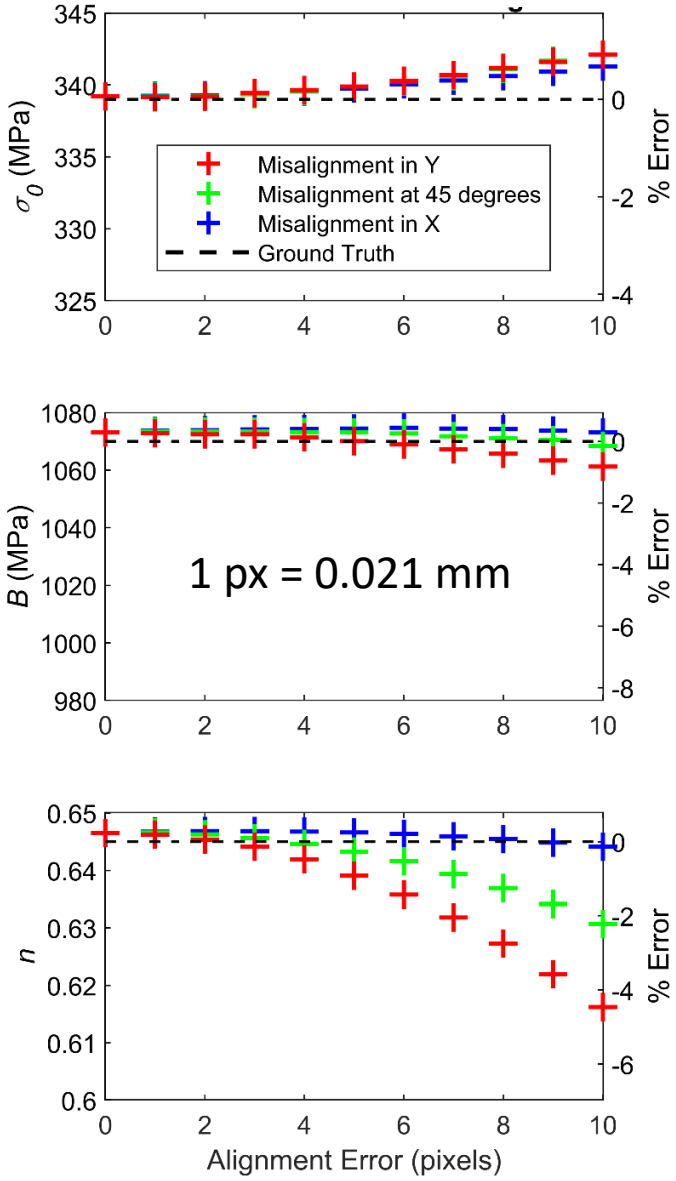

Fiducial markings for better alignment of DIC data to FE model

Vicker's microhardness machine with micrometer translation stages

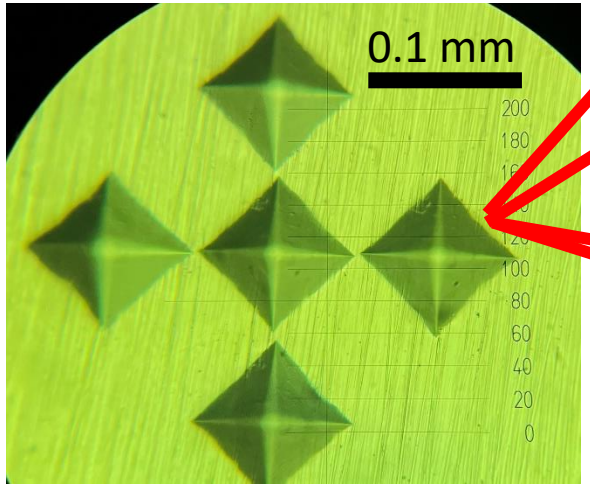

20 µm deep indentions

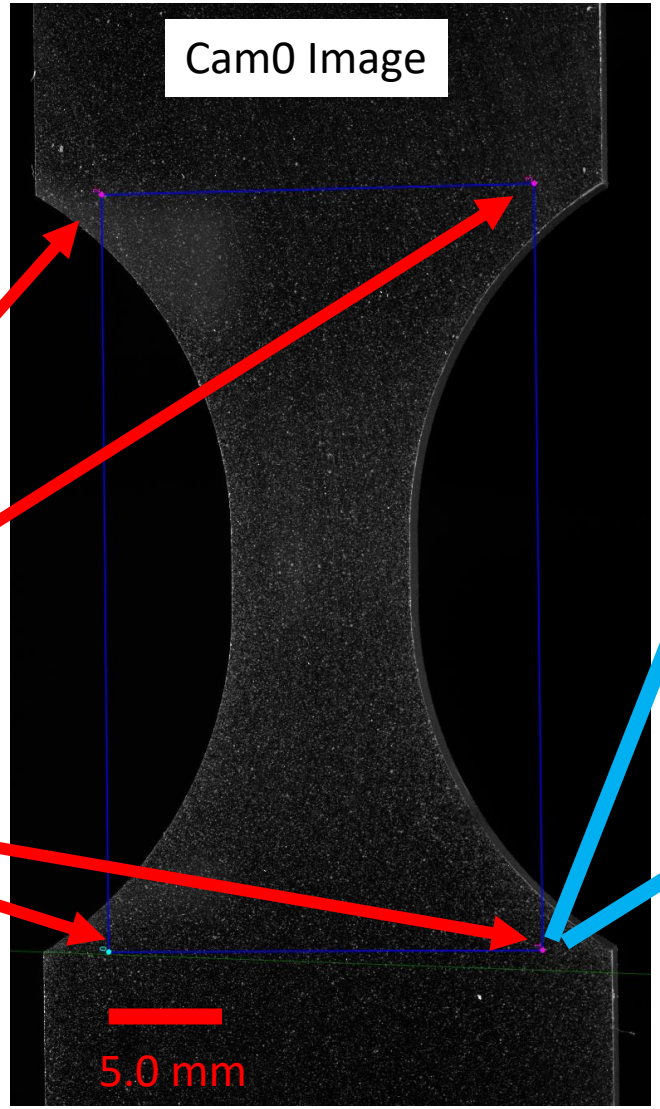

Cam0

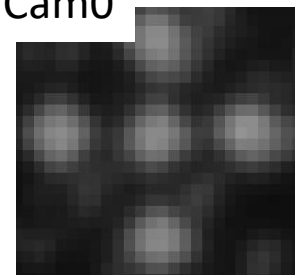

Cam1

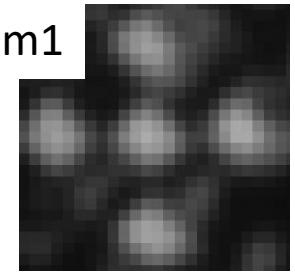

Similar pattern recovered in both cameras

Experimental/Metrological

- DIC filtering biases → Levelling the FE Model
- Misalignment between DIC and FE model → Fiducials
- → Non-ideal boundary conditions←
- DIC errors such as image noise, pattern-induced bias, subpixel interpolation bias whose effects are small on calibration (Fayad 2022)

Model Form Error

- Assumptions of Plane Stress (Future work)
- Selection of Empirical Models (Future work)

Inverse Technique

- Choice of Cost Function quantities for the Inverse Method (Future work)

Non-Ideal Boundary Conditions in Validation Studies

Experiment

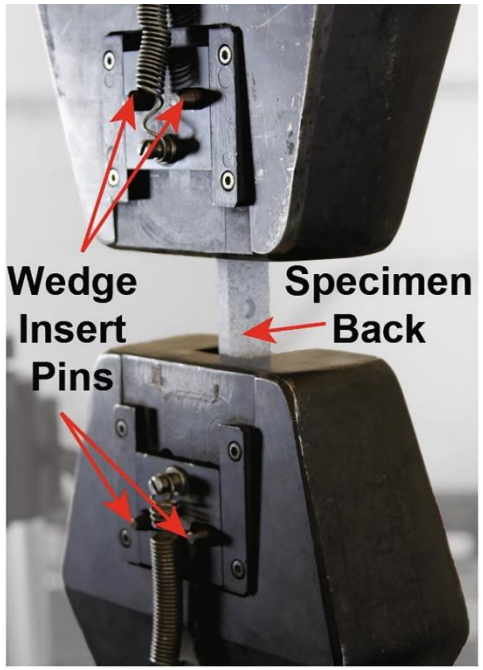

Uniaxial extension of a tensile specimen with a blind hole
(EMC Jones et al. 2018)

Modeling and Validation

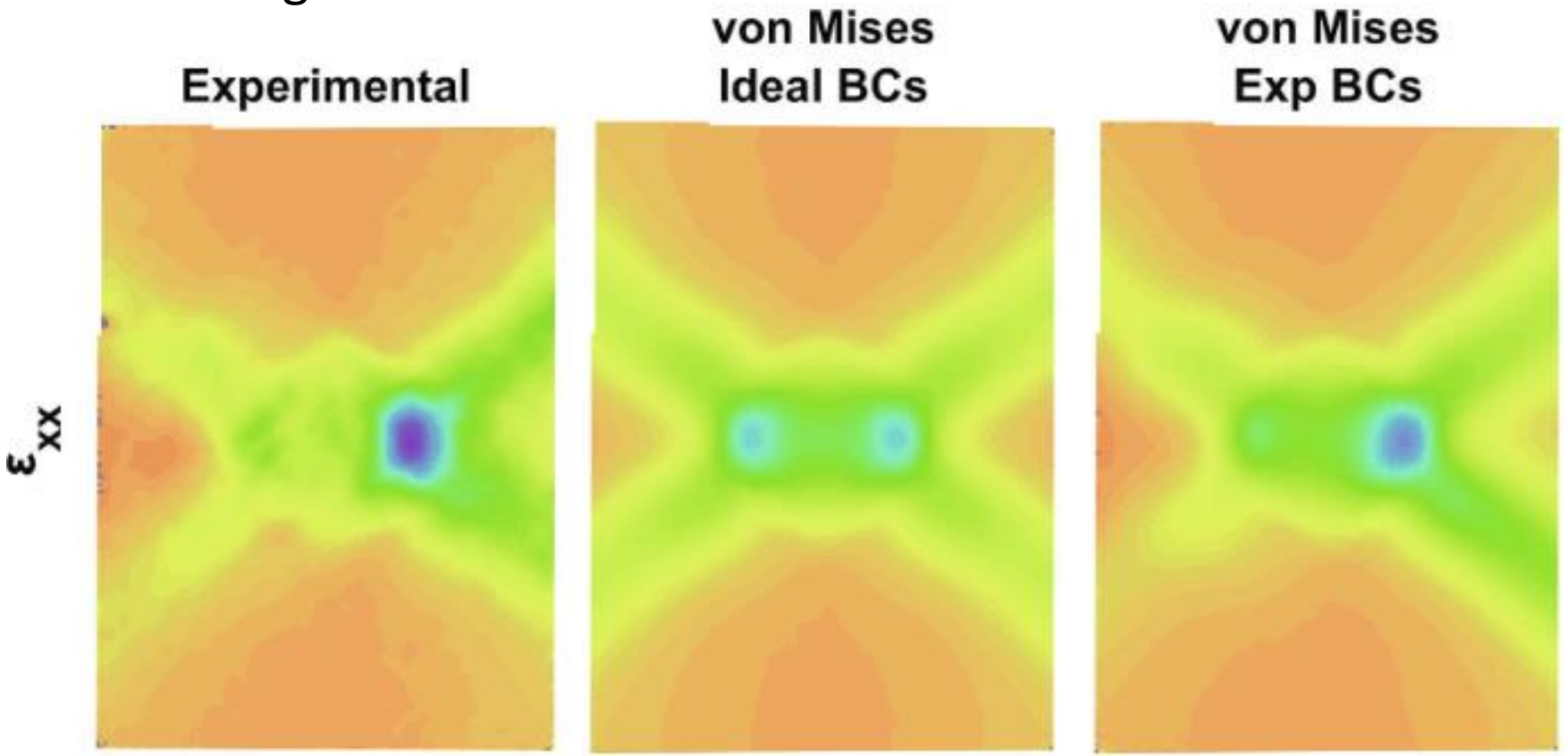

Asymmetric grip behavior

Asymmetry not replicated by FEA

Asymmetry captured by FEA

Using Experimentally measured BCs in FEA

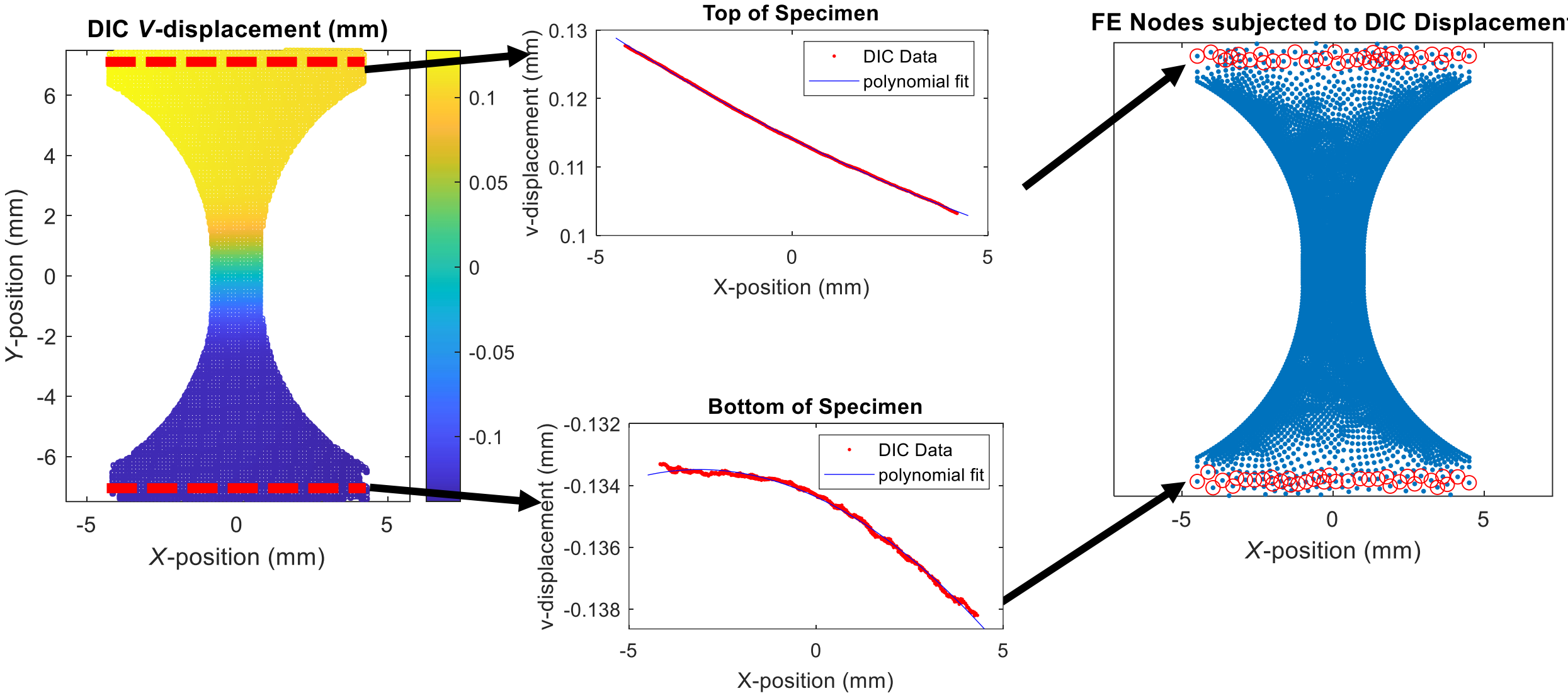

Using Experimentally vs Ideal BCs in FEA

$$\chi^2(\boldsymbol{\rho}) = \underbrace{\sum_{\Omega_{exp}}\left[E_{exp} - E_{FEA}(\boldsymbol{\rho})\right]^2}_{\chi_E^2} + \underbrace{\frac{1}{\gamma_f^2}\left(F_{exp} - F_{FEA}(\boldsymbol{\rho})\right)^2}_{\chi_F^2}$$

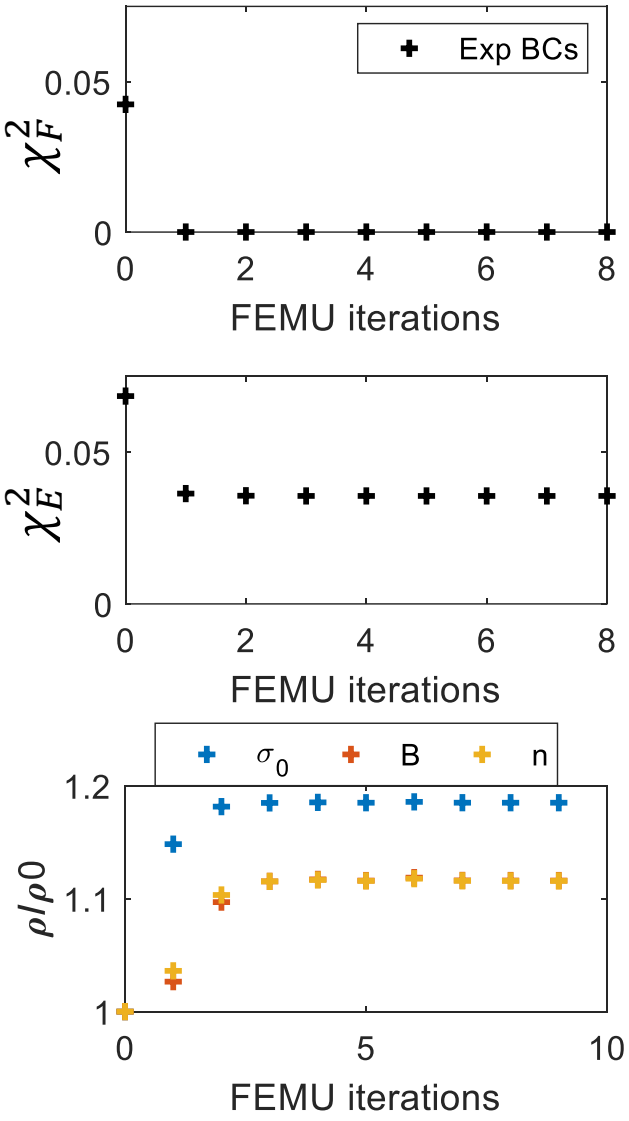

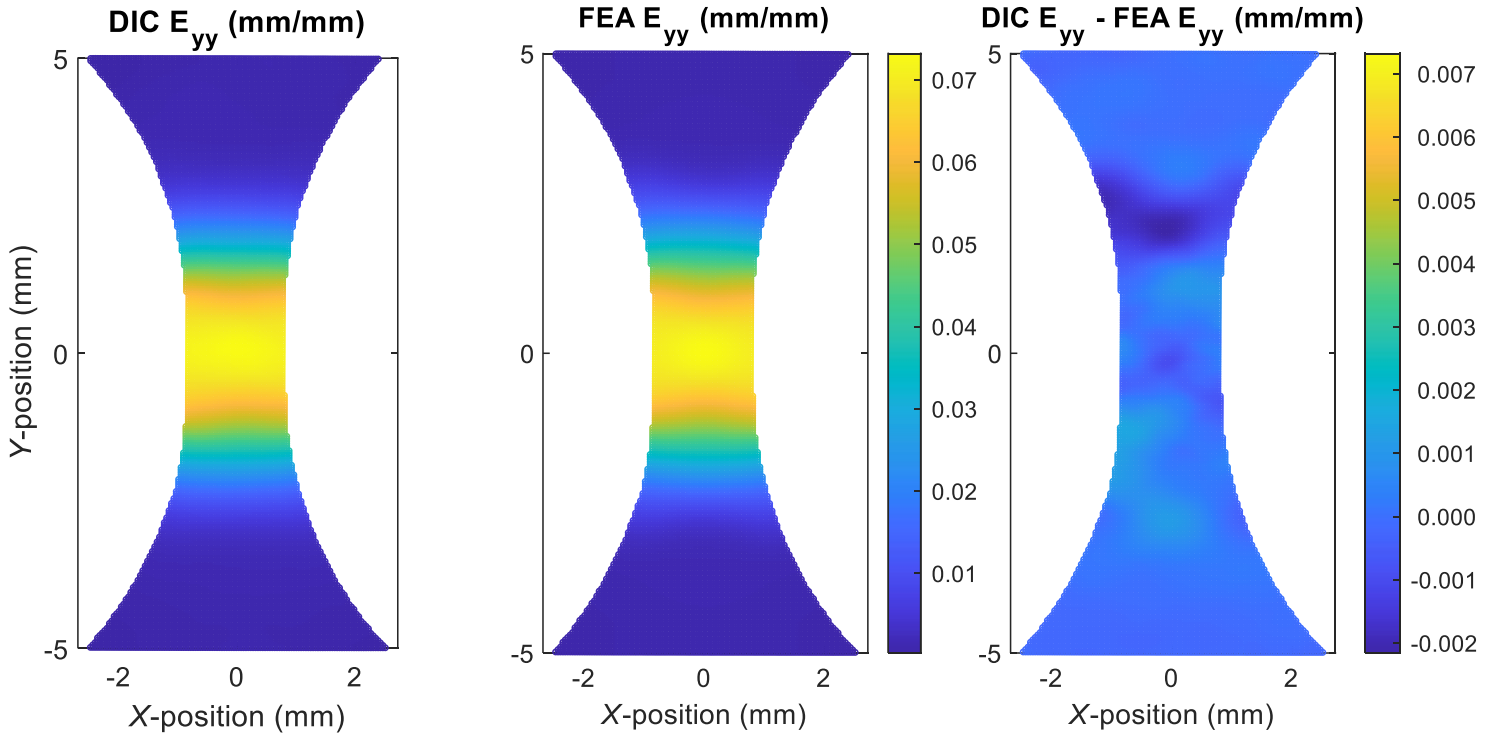

	σ_0 (MPa)	B (MPa)	n	χ_F^2	χ_E^2
Ideal BCs	299.1	1,188	0.6458	0.0000	0.0383
Measured BCS	301.3	1,194	0.6477	0.0000	0.0355

Summary

- **DIC filtering biases → Levelling the FE Model**
- **Misalignment between DIC and FE model → Fiducials**
- **Non-ideal boundary conditions → Experimentally measured BCs**

Future Work

- Calibration using hourglass specimen
- Validation test series of a complex geometry
- Quantitative assessment of various error sources using FEMU and DIC

Experimental set-up at the University of Illinois

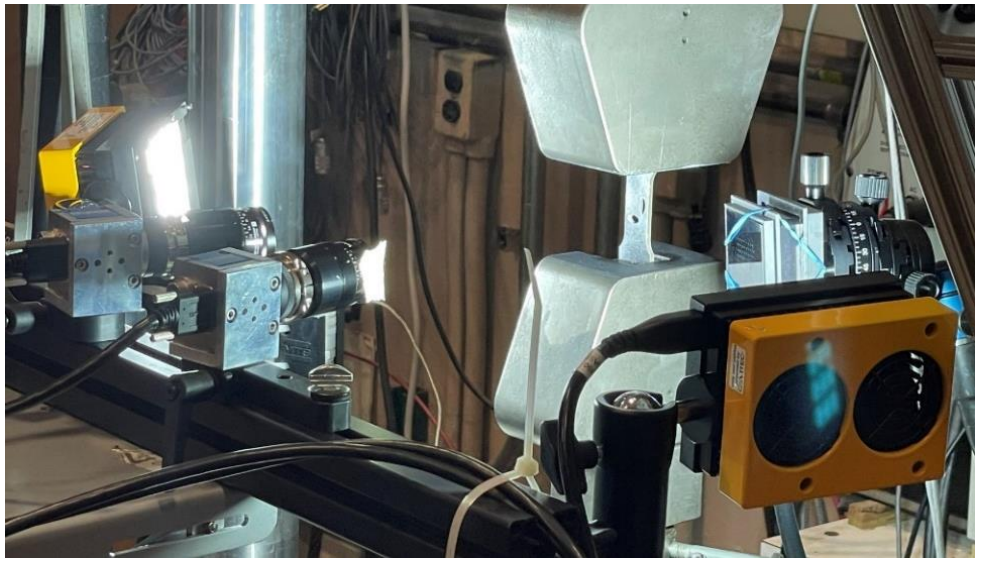

Validation specimen